Journal of Neurochemistry, 2005, **94**, 1728–1738 doi:10.1111/j.1471-4159.2005.03334.x

Evidence for low GluR2 AMPA receptor subunit expression at synapses in the rat basolateral amygdala

Divina S. Gryder,[1] Dora C. Castaneda[1,2] and Michael A. Rogawski

Epilepsy Research Section, National Institute of Neurological Disorders and Stroke, National Institutes of Health, Bethesda, Maryland, USA

Abstract

Fast excitatory synaptic responses in basolateral amygdala (BLA) neurons are mainly mediated by ionotropic glutamate receptors of the α-amino-3-hydroxy-5-methylisoxazole-4-propionate (AMPA) subtype. AMPA receptors containing an edited GluR2 subunit are calcium impermeable, whereas those that lack this subunit are calcium permeable and also inwardly rectifying. Here, we sought to determine the extent to which synapses in the rat BLA have AMPA receptors with GluR2 subunits. We assessed GluR2 protein expression in the BLA by immunocytochemistry with a GluR2 subunit-specific antiserum at the light and electron microscopic level; for comparison, a parallel examination was carried out in the hippocampus. We also recorded from amygdala brain slices to examine the voltage-dependent properties of AMPA receptor-mediated evoked synaptic currents in BLA principal neurons. At the light microscopic level, GluR2 immunoreactivity was localized to the perikarya and proximal dendrites of BLA neurons; dense labeling was also present over the pyramidal cell layer of hippocampal subfields CA1 and CA3. In electron micrographs from the BLA, most of the synapses were asymmetrical with pronounced postsynaptic densities (PSD). They contained clear, spherical vesicles apposed to the PSD and were predominantly onto spines (86%), indicating that they are mainly with BLA principal neurons. Only 11% of morphological synapses in the BLA were onto postsynaptic elements that showed GluR2 immunoreactivity, in contrast to hippocampal subfields CA1 and CA3 in which 76% and 71% of postsynaptic elements were labeled ($p < 0.001$). Synaptic staining in the BLA and hippocampus, when it occurred, was exclusively postsynaptic, and particularly heavy over the PSD. In whole-cell voltage clamp recordings, 72% of BLA principal neurons exhibited AMPA receptor-mediated synaptic currents evoked by external capsule stimulation that were inwardly rectifying. Although BLA principal neurons express perikaryal and proximal dendritic GluR2 immunoreactivity, few synapses onto these neurons express GluR2, and a preponderance of principal neurons have inwardly rectifying AMPA-mediated synaptic currents, suggesting that targeting of GluR2 to synapses is restricted. Many BLA synaptic AMPA receptors are likely to be calcium permeable and could play roles in synaptic plasticity, epileptogenesis and excitoxicity.

Keywords: AMPA receptor, basolateral amygdala, electron microscopy, GluR2 subunit, hippocampus, patch clamp recording.

J. Neurochem. (2005) **94,** 1728–1738.

Ionotropic glutamate receptors of the α-amino-3-hydroxy-5-methylisoxazole-4-propionate (AMPA) subtype are the main mediators of fast excitatory synaptic transmission in the basolateral amygdala (BLA) (Li and Rogawski 1998; Li *et al*. 2001), as in other regions of the central nervous system (Dingledine *et al*. 1999). Functional AMPA receptors are homo- or heterotetramers of four protein subunits, GluR1–4. Of these, the GluR2 subunit plays a crucial role in controlling the calcium permeability of AMPA receptors. GluR2 mRNA ordinarily undergoes post-transcriptional editing so that the expressed protein contains a positively-charged arginine in place of the gene-encoded glutamate at a critical position in the M2 membrane loop that forms the lining of the AMPA

Received April 8 2005; revised manuscript received May 15, 2005; accepted May 18, 2005.

Address correspondence and reprint requests to Michael A. Rogawski, M.D., Ph.D., Epilepsy Research Section, NINDS, NIH, Porter Neuroscience Research Center, Building 35, Room 1C-1002, 35 Convent Drive MSC 3702, Bethesda, MD 20892–3702, USA.
E-mail: michael.rogawski@nih.gov

[1]D. S. Gryder and D. C. Castaneda contributed equally to this work.
[2]The present address of D. C. Castaneda is Stanford University School of Medicine, 300 Pasteur Drive, Stanford, CA 94305, USA.

Abbreviations used: aCSF, artificial cerebrospinal fluid; BLA, basolateral amygdala; EC, external capsule; PBS, phosphate-buffered saline; PSD, postsynaptic densities; RI, rectification index; s-aCSF, sucrose-based artificial CSF.

receptor's pore. AMPA receptors lacking an edited GluR2 subunit have substantial calcium permeability and also exhibit inward rectification, whereas the presence of a single GluR2 subunit is sufficient to maximally reduce calcium permeability (Geiger *et al*. 1995). Principal neurons in many forebrain regions, including the hippocampus and neocortex, contain such edited GluR2 subunits, so that AMPA receptor-mediated synaptic transmission in these neurons does not involve appreciable calcium entry. In contrast, AMPA receptors in interneurons in these regions may have a low abundance of GluR2 (Jonas and Burnashev 1995), and the synaptic responses mediated by these AMPA receptors are inwardly rectifying and have substantial calcium permeability (McBain and Dingledine 1993; Jonas *et al*. 1994; Geiger *et al*. 1995, 1997). Recently, however, it has become recognized that some neurons, such as spinal motoneurons (and probably also many interneurons; Vissavajjhala *et al*. 1996), may have a substantial complement of calcium-permeable AMPA receptors, even though they contain considerable GluR2 mRNA and express GluR2 protein (Greig *et al*. 2000). Therefore, AMPA receptor subunits within a neuron are not always free to combine; rather, distinct populations of heteromeric channels can be formed, allowing for the existence of a population of AMPA receptors lacking GluR2 in cells that synthesize appreciable GluR2.

Neurons in the BLA receive excitatory glutamatergic inputs from cortical and subcortical regions (Rainnie *et al*. 1991; Gean and Chang 1992). Golgi studies have demonstrated two main cell types in the BLA: (i) principal neurons: large pyramidal neurons with spiny dendrites that project outside the BLA (class I cells); and (ii) interneurons: aspinous, predominantly GABAergic non-pyramidal local circuit neurons (class II cells) (McDonald 1982; Millhouse and DeOlmos 1983; McDonald 1984, 1992a,). Principal neurons constitute 85% of the total neuronal population of the BLA (McDonald 1992b). Both principal neurons and interneurons receive extrinsic glutamatergic inputs. Fast excitation of principal neurons is mainly mediated by AMPA receptors, with additional components due to NMDA and kainate receptors (Li and Rogawski 1998; Li *et al*. 2001).

It has previously been reported that principal neurons in the BLA express high levels of immunoreactivity with a GluR2/3 (McDonald 1994, 1996; Farb *et al*. 1995) or GluR2 (He *et al*. 1999)-specific antibody, whereas non-pyramidal cells either lack GluR2 immunoreactivity (McDonald 1994, 1996) or at least have synaptic AMPA receptors with a reduced complement of GluR2 subunits compared with synapses onto principal neurons (He *et al*. 1999). Moreover, some pyramidal neurons in the BLA exhibit AMPA receptors with linear current–voltage relationships, whereas AMPA receptor responses in interneurons show marked inward rectification (Mahanty and Sah 1998). These studies raise the possibility that the principal neurons in the BLA may largely express calcium-impermeable AMPA receptors. In the present study, this issue was re-evaluated using a GluR2 subunit-specific antibody to assess the expression of the GluR2 subunit in BLA synapses at the ultrastructural level, and with whole-cell voltage clamp recordings from BLA principal neurons to determine the rectifying properties of AMPA receptors in these cells.

Materials and methods

Immunocytochemistry

Tissue preparation

Male adult (9–12-week-old; 300–400 g) Sprague-Dawley rats were anesthetized by intraperitoneal injection with a mixture of 60 mg/kg ketamine and 10 mg/kg xylazine in 0.9% saline, and perfused via the ascending aorta with 50 mL 0.9% saline followed by 500 mL of a fixative containing 4% paraformaldehyde and 0.25% glutaraldehyde. Brains were removed and post-fixed in the same fixative for 3 h at 4°C. Following extensive washing with 0.1 M phosphate-buffered saline (PBS; pH 7.4) containing 15% sucrose for 48 h (4°C), the brains were frozen and stored at −80°C. Animal procedures were carried out in strict compliance with institutional regulations and the Guide for the Care and Use of Laboratory Animals of the National Research Council (National Academy Press, Washington, DC; http://www.nap.edu/readingroom/books/labrats/).

GluR2 immunostaining

Coronal frozen sections (100 μm) containing the BLA and hippocampal subfields CA1 and CA3 were cut with a vibrating slicer (Vibratome, St Louis, MO, USA) and collected in cold PBS. Immunoperoxidase labeling was carried out with an affinity-purified goat polyclonal IgG antiserum raised against a synthetic peptide corresponding to a 20-amino acid sequence identical to residues 861–880 in the carboxy terminus of rat GluR2 (QNSQNFATYKEGYNVYGIES; Santa Cruz Biotechnology, Santa Cruz, CA, USA). The antibody was confirmed to react with GluR2 by immunohistochemistry and western blotting with rat and mouse brain extracts. Western blots revealed the labeling of a single band, with a molecular weight of approximately 109 kDa, corresponding with the predicted molecular mass of GluR2 and the mass of the fully processed protein in brain and transfected heterologous cells (Hall *et al*. 1997; Janssens and Lesage 2001). The antibody reacts to a much lesser extent with GluR3, which has 78% homology to 19 amino acids of the immunogen. There was no cross-reactivity to other AMPA receptor subunits. In agreement with this pattern of specificity, the antibody was found to react specifically with SK-N-SH cells that express GluR2 and GluR3, but not GluR1 (Yoshioka *et al*. 1996). After thoroughly washing with PBS, the free-floating sections were incubated at 4°C for 3 days, with the antiserum diluted 1 : 250 in 0.01 M PBS (pH 7.4) containing 0.3% Triton X-100 (Sigma, St Louis, MO, USA) and 1% normal goat serum. For light and electron microscopy, the immunoreaction product was visualized according to the avidin-biotin complex (ABC) method using the Vectstatin elite ABC kit (Vector Laboratories, Burlingame, CA, USA) and 3,3′-diaminobenzidine as chromogen, which produces a black reaction product. The sections were thoroughly

washed and stored in PBS before further processing. Experiments for antibody specificity were performed in adjacent sections by (i) omission of the GluR2-specific antibody, and (ii) pre-adsorption of the anti-GluR2 antibody with the antigenic peptide at 4°C for 24 h. In both cases, immunostaining was completely eliminated (see Results).

Preparation for electron microscopy

Sections prepared for electron microscopy were immersion fixed with 4% glutaraldehyde at room temperature for 1–2 h, followed by washing in PBS (pH 7.4) three times for 10 min each. The sections were post-fixed in 1% osmium tetroxide for 1 h, washed three times for 10 min each in cold acetate buffer and then exposed to uranyl acetate overnight to improve the contrast in the electron microscope. The sections were washed in cold acetate buffer three times for 10 min each and dehydrated in increasing concentrations of ethanol. Following the dehydrations, the sections were infiltrated in propylene oxide two times, 15 min each, and then overnight on a rotator with 50/50 propylene oxide/epoxy resin. The sections were flat embedded in 100% epoxy resin on plastic Thermonox coverslips, polymerized in a 50°C oven overnight and later placed in a 60°C oven for 48 h. Under light microscopic examination, the BLA, and CA1 and CA3 of the hippocampus, were cut out from the slides and glued onto resin blocks with cyanoacrylate adhesive. Ultrathin sections were cut parallel to the block surface with a DSK microslicer (Ted Pella, Redding, CA, USA) and collected on polyvinyl butyral (Pioloform)-coated, single slot gold grids. Each thin section was approximately 70 nm thick and all sections used in the analysis were within 1–2 μm of the surface, well within the range of penetration of the antibody. Sections were viewed at a magnification of 15 000–40 000 and photographed with a JEOL 1200 EX electron microscope (JEOL, Peabody, MA, USA).

Quantitative analysis of electron microscopy

To characterize the synaptic localization of GluR2 antibody labeling, a series of electron micrographs was taken randomly in the areas of interest (BLA, and hippocampal subfields CA1 and the mossy fiber area of CA3). Prior to the analysis of the micrographs, four conditions were set for the scoring of morphological synapses according to labeling with the immunoperoxidase reaction product: (i) presynaptic and postsynaptic, (ii) only presynaptic, (iii) only postsynaptic or (iv) no labeling. Each electron micrograph was then scored blind. Since immunoperoxidase is a diffusible marker, no attempt was made to quantitatively assess localization of the reaction product within the presynaptic or postsynaptic compartments, or specifically to synapses. Each category was summed among all micrographs and the categories were compared using a χ^2 goodness of fit test. Lower and upper limits of the 95% confidence interval for proportions were determined using VassarStats (http://faculty.vassar.edu/lowry/VassarStats.html). Synapses were also scored for the type of postsynaptic element: dendritic shaft, dendritic spine or cell body. Dendritic shafts were distinguished by their large size and enrichment in mitochondria and microtubules. Dendritic spines were recognized by their bulbous appearance, lack of mitochondria and absence of microtubles. Spines frequently received asymmetric synaptic inputs. Cell bodies (perikarya) had Golgi apparatus, endoplasmic reticulum and nuclei.

Electrophysiology

Slice preparation and perfusion

Male 20–30-day-old Sprague-Dawley rats were anesthetized with halothane, decapitated, and the brain quickly removed and immersed in ice-cold (4°C), sucrose-based, artificial cerebrospinal fluid (s-aCSF) solution containing (in mM): 200 sucrose, 3 KCl, 1.25 Na_2PO4, 26 $NaHCO_3$, 10 glucose, 1 $MgCl_2$ and 2 $CaCl_2$ oxygenated with a mixture of 95% O_2−5% CO_2 (pH 7.4; 300 mOsm/L). Juvenile rats were used for electrophysiology because slice viability and neuron accessibility for whole-cell recording is greater than with slices from mature animals. After incubating in the s-aCSF solution for 90 s, coronal 450 μm sections were cut from one hemisphere using a vibrating slicer (Vibratome). The three slices containing the BLA immediately rostral to the lateral ventricles were collected for recording. An additional three slices were later obtained from the second hemisphere. The slices were incubated for 1 h in an incubation chamber of warmed (36°C), continuously oxygenated (95% O_2−5% CO_2) artificial cerebrospinal fluid (aCSF) identical in composition to s-aCSF except that 130 mM NaCl replaced the sucrose. After recovery, individual slices were transferred to a recording chamber mounted on the stage of an upright microscope (Axioskop II, Carl Zeiss, Thornwood, NJ, USA). The slices were held in place with a 1 mm diameter platinum wire and were visualized by IR-DIC microscopy using a 40 × water immersion objective. The recording chamber was continuously perfused at a rate of 3–4 mL/min with warmed aCSF (24–25°C) using a gravity fed fluid delivery system.

Whole-cell recording

Patch pipette electrodes were pulled from borosilicate glass tubing (M1B150F-4, WPI, Sarasota, FL, USA) and had a resistance of 5–7 MΩ when filled with intracellular solution consisting (in mM) of: 140 cesium methanesulfonate, 10 HEPES, 10 EGTA, 11 NaCl, 0.5 $CaCl_2$, 1 Mg_2Cl, 2 NaATP and 0.2 NaGTP (pH 7.28; 285 mOsm/L). Lidocane *N*-ethyl bromide quarternary salt (QX314; 5 mM) was added to the pipette solution to prevent generation of Na^+-dependent action potentials caused by a poor control of the membrane potential. Spermine (100 μM) was also added to the intracellular recording solution to maintain adequate intracellular polyamines so as to preserve inward rectification of calcium-permeable AMPA receptor currents (Donevan and Rogawski 1995; Kamboj *et al.* 1995). The recording electrode was positioned near the white matter tract demarcating the medial extent of the BLA. Tight seal (>10 GΩ), whole-cell, voltage clamp recordings were obtained from the somata of principal neurons in the BLA using an Axopatch 1D amplifier (Axon Instruments, Foster City, CA, USA). The cell membrane was broken into at a holding potential of −60 mV and capacitance compensation was applied. Access resistance was regularly monitored. No cleaning of the cell somata was performed. Recordings were made from the middle of the region presumed to represent the BLA (between the amygdalar capsule and stria terminalis) so as to avoid interneurons that are clustered at the borders of the nucleus (McDonald 1984). Principal neurons were identified by oval, conical or pyramidal-shaped soma (>10 μm in the longest extent) and a large apical dendritic trunk arising from the soma (Washburn and Moises 1992). The identity of some neurons with these characteristics was confirmed morphologically after filling with 0.5% biocytin.

Stimulation

Synaptic responses were evoked using a bipolar tungsten electrode (A-M Systems, Carlsborg, WA, USA) placed in the 'external capsule' (EC) (actually the amygdalar capsule according to Swanson and Petrovich 1998). The site of stimulation was at the inferiormost extent of the visible portion of the amygdalar capsule, immediately lateral to the BLA. Square, 100 μs duration, unipolar pulses were applied via a constant-current isolation unit (Cygnus Technology, Delaware, PA, USA) at an intensity of 700–900 μA to elicit a maximum synaptic response (typically >500 pA peak amplitude). The stimulation was routinely applied at 0.1 Hz. Synaptic currents were routinely recorded at −70 mV, except as noted.

Isolation of AMPA receptor currents

AMPA receptor-mediated currents were isolated by switching to aCSF supplemented with (in μM): 100 AP5 [(D(−)-2-amino-5-phosphonopentanoic acid)] (Tocris Cookson, St Louis, MO, USA), 10 LY 293558 {(3S,4aR,6R,8aR)-6-[2-(1(2)H-tetrazole-5-yl)ethyl]-decahydroisoquinoline-3-carboxylic acid}, 10 (−)-bicuculline methiodide (Sigma) and 10 SCH 50911 (Tocris Cookson) to block NMDA, kainate, $GABA_A$ and $GABA_B$ receptor currents, respectively. In some experiments, the identity of AMPA receptor-mediated synaptic currents was verified by addition of 50 μM GYKI 52466 [1-(4-aminophenyl)-4-methyl-7,8-methylenedioxy-5H-2,3-benzodiazepine hydrochloride)] (RBI, Natick, MA, USA) to the perfusion solution. Solution exchange was accomplished by closing the valve containing the control solution and opening another valve containing the antagonist solution. LY 293558 was a generous gift of Eli Lilly (Indianapolis, IN, USA).

Data analysis

Currents were acquired using Clampex 8.03 (Axon Instruments) at a sampling rate of 4 or 5 kHz, and were filtered using a 4-pole Bessel filter with a corner frequency of 2 kHz and 80 db/decade attenuation. The signals were stored directly to a computer hard disk for later analysis using Clampfit (Axon Instruments). Origin (OriginLab, Northampton, MA, USA) was used for final plotting. The rectification index (RI) was calculated according to the formula of Ozawa *et al*. (1991): $RI = [I_{+40}/(40 - E_{rev})]/[I_{-60}/(-60 - E_{rev})]$ where I_{+40} and I_{-60} are the peak amplitudes of the synaptic currents at +40 and −60 mV, respectively, and E_{rev} is the reversal potential determined for the cell under study. Rectification index values < 1 indicate inward rectification.

Results

Light microscopic distribution of GluR2 immunoreactivity

Specific GluR2 staining was diffusely distributed throughout the neuropil in the regions examined, and concentrated over many neuronal perikarya and their proximal dendrites. Within the hippocampal formation, staining was especially prominent over the pyramidal cell layer in subfields CA3 and CA1 (Fig. 1a–c). Neurons with GluR2 immunoreactivity were seen in the amygdala and the adjacent piriform cortex (Fig. 1d). The BLA was densely packed with darkly stained neurons (Fig. 1e). The stained neurons were oval or pyramidal-shaped,

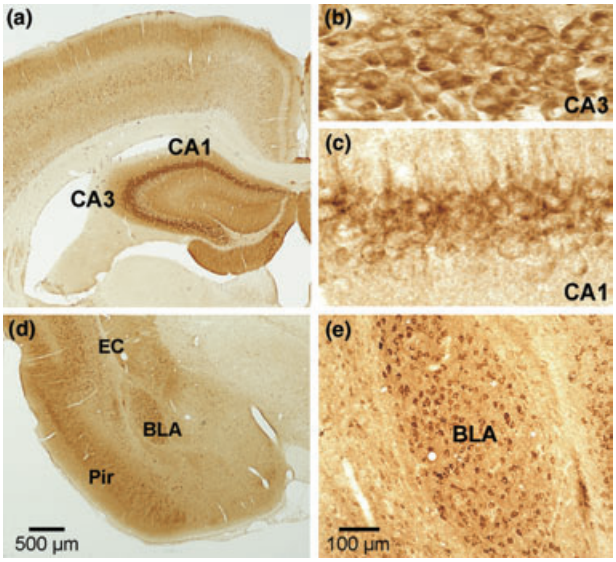

Fig. 1 Immunocytochemical localization of GluR2 AMPA receptor subunit immunoreactivity in the hippocampus and amygdala. (a) Low power light microscopic view of hippocampus and surrounding neocortex. Note the dense antibody staining of pyramidal cells in the CA3 and CA1 subfields. (b), (c) Higher power view of GluR2 immunolabeling of neuronal cell bodies and processes in CA3 (b) and CA1 (c). (d) Low power view of the anterior portion of the amygdala showing the external capsule (EC) and piriform cortex (Pir). (e) Higher power view of the BLA. Scale in (d) also applies to (a).

with a largest dimension of 18.7 ± 2.1 μm and a smallest dimension of 14.4 ± 1.5 μm (mean ± SD; $n = 30$). At higher power, the reaction product appeared to be mainly concentrated in the perikarya, and in one to three proximal dendritic shafts in the plane of the section (Figs 2a and b1). The nuclei of labeled neurons were devoid of immunoreactivity. The surrounding neuropil exhibited less staining than in the neuropil of the hippocampal pyramidal layer, which was also more densely packed with cell bodies (Figs 1b and c). Tissue processed for electron microscopy was osmicated, producing darker brown-black staining. As shown in Fig. 3, this intense staining was completely eliminated by preadsorption of the antiserum with the immunogen.

Electron microscopic distribution of GluR2 immunoreactivity

The reaction product generated by specific GluR2 antibody binding consisted of small granules measuring 100 nm or less. In both the hippocampus and amygdala, electron microscopy revealed a non-uniform distribution of labeling, with a predominance of labeling confined to dendrites (including dendritic shafts) and spines (Figs 4 and 5a). In addition, reaction product was seen in patches in the cell body, often along the endoplasmic reticulum and adjacent to the nuclear envelope (Fig. 2b2). Glial processes and presynaptic terminals were never stained. Within dendrites and

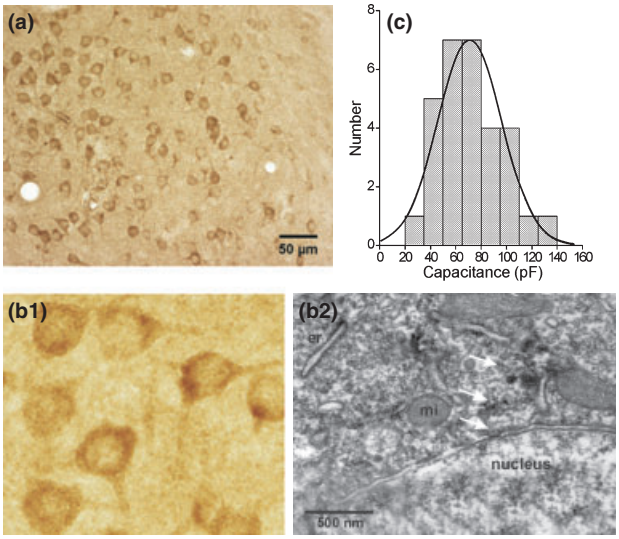

Fig. 2 Uniform perikaryal GluR2 staining of BLA neurons and homogeneity of cell capacitance measurements. (a) Light microscopic view of immunocytochemical staining in BLA showing labeling of similar sized perikarya. (b1) Detail from (a). (b2) Electron micrograph of a stained neuronal perikaryon in the BLA. White arrows indicate clumps of reaction product in the cytoplasm. er, Endoplasmic reticulum; mi, mitochondrion. (c) Distribution of cell capacitance values from whole-cell voltage clamp recordings. Solid line shows best Gaussian fit to the data (mean, 66.7 pF; standard deviation, 45.5 pF).

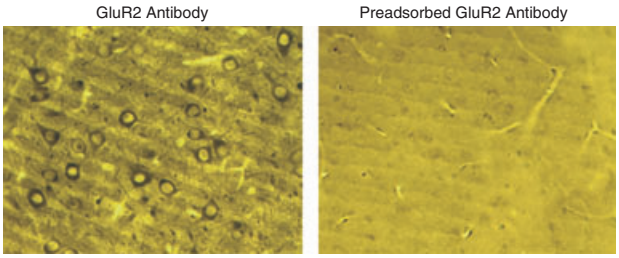

Fig. 3 Light micrograph of BLA sections processed for electron microscopy prior to embedding. Images are from adjacent sections processed with GluR2-specific antiserum (left) and GluR2 antiserum pre-adsorbed with the immunogenic peptide (right). Pre-adsorbed antiserum similarly showed no reactivity in hippocampus (not shown).

spines, uniform clumps of reaction product usually filled the entire membrane-delimited dendritoplasm, excluding mitochondria which were not stained. Labeling was especially dense over the postsynaptic elements of synapses, with labeling of postsynaptic densities apposed to unlabeled presynaptic terminals that were filled with finely distinguished round vesicles. The postsynaptic densities were typically the most heavily stained structures within dendrites and spines. In areas CA3 and CA1, most of the spine synapses originated from basal and apical dendrites of pyramidal cells. In the BLA, synapses were much less often labeled (Figs 4c1 and 5b1–5). However, when staining was

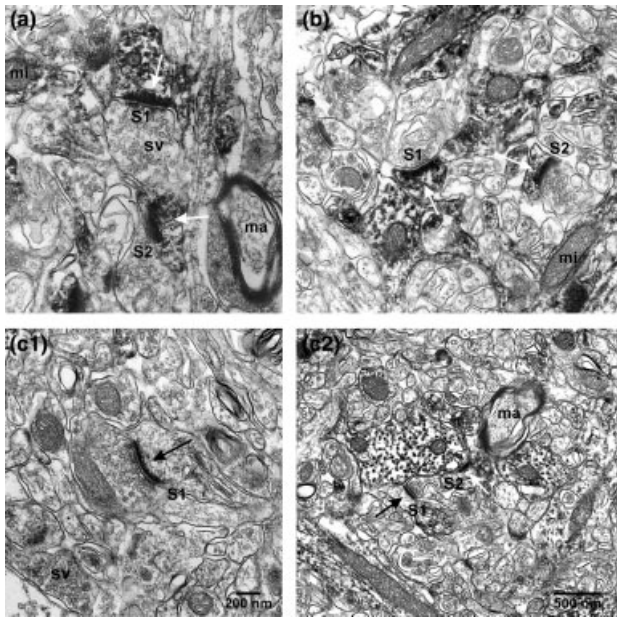

Fig. 4 Electron microscopic localization of GluR2 immunoreactivity in rat hippocampal subfields CA3 and CA1, and in the BLA. (a) Immunoperoxidase reaction product at two mossy fiber synapses (S1, S2) in the CA3 region. White arrows indicate staining of the postsynaptic membranes and postsynaptic densities. In addition, granular electron-dense reaction product is uniformly distributed within the membrane-delimited postsynapic elements. The stained postsynaptic elements are apposed to unstained presynaptic terminals containing clear, round synaptic vesicles (sv). (b) Two stained synapses (S1, S2) in the CA1 region of hippocampus (white arrows). (c1) Unstained synapse (S1) in the BLA. Black arrow points to postsynaptic elements lacking reaction product. (c2) Another example from the BLA showing two synapses, one of which (S1) is unlabeled (black arrow shows unlabeled postsynaptic elements) and the second (S2) is apposed to a large labeled postsynaptic structure (white arrow). mi, Mitochondrion; ma, myelinated axon. Scale bar in (c1) applies to (a); scale bar in (c2) applies to (b).

present, it appeared much the same as in the hippocampal regions; patches of reaction product filled the entire extent of the dendrite and the postsynaptic density was especially darkly stained (Figs 4c2 and 5a).

Synapses within photomicrographs of hippocampal subfields CA1 and the mossy fiber region of CA3, and the BLA, were scored for the presence of presynaptic and postsynaptic labeling. Presynaptic labeling was not observed. In area CA3 of the hippocampus, 469 synapses were analyzed. Of the total, 334 synapses exhibited postsynaptic labeling and the remainder were unlabeled (Fig. 6). In area CA1, 459 synapses were analyzed and 351 were labeled postsynaptically. In contrast, only 64 synapses among 560 in BLA exhibited GluR2 postsynaptic labeling. Thus, in the CA3 and CA1 samples, 71.2% (95% CI: 66.7–75.1%) and 76.5% (95% CI: 72.4–80.1%) of synapses exhibited postsynaptic labeling, whereas in the BLA, the fraction was 11.5% (95% CI: 9.1–14.4%).

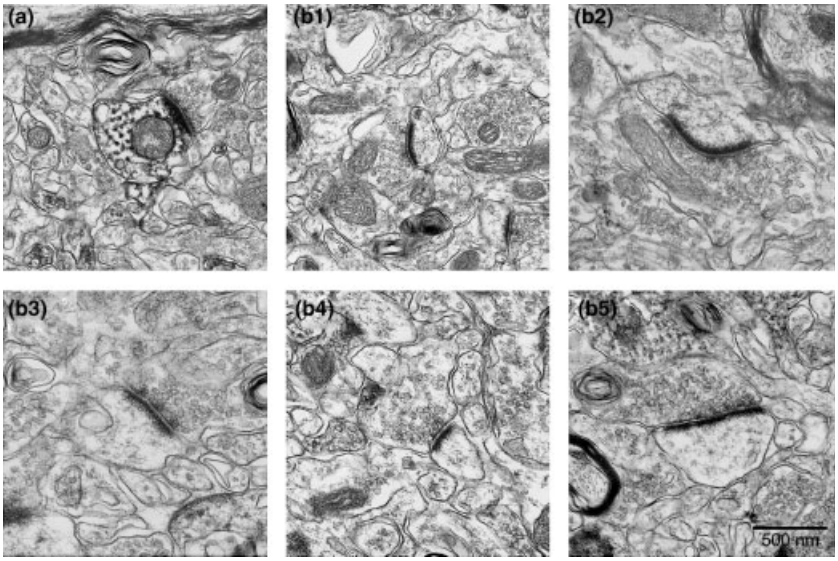

Fig. 5 Representative synapses from rat BLA sections processed for GluR2 immunoreactivity. (a) Rare synapse demonstrating postsynaptic GluR2 labeling. (b1–5) Samples of more commonly observed unlabeled synapses. Scale in (b5) applies to all panels.

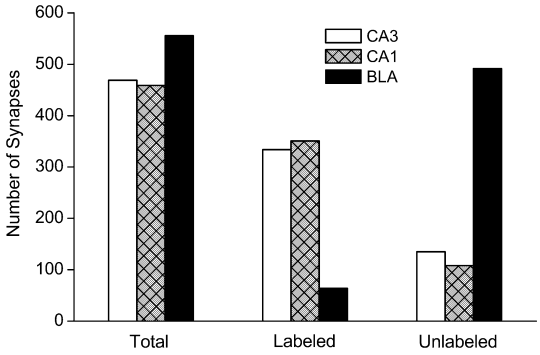

Fig. 6 Comparison of synaptic labeling in hippocampal subfields CA3 and CA1, and BLA. Synapses in electron micrographs were scored for labeling postsynaptically, presynaptically, both or none. No labeling was observed presynaptically. The bars indicate the total number of synapses analyzed in each of the three regions, and the distribution among those that were labeled postsynaptically and those that were unlabeled. A χ^2 goodness of fit test on a 3×2 contingency table revealed a non-uniform distribution of synapses labeled with GluR2 postsynaptically among the three brain regions surveyed ($p < 0.001$, $\chi^2 = 542$, 2 degrees of freedom). Pairwise analysis indicated differences between the BLA and each of the two hippocampal regions ($p < 0.001$) but no significant difference between the two hippocampal regions ($p > 0.08$).

Of the 560 synapses in the BLA area that were analyzed, 86% (480) were on dendritic spines and the remainder were on dendritic shafts. Perikaryal synapses were not observed. Of the 64 synapses in the BLA that showed postsynaptic GluR2 labeling, 77% (49) were on spines and the remainder were on dendritic shafts.

Passive properties of BLA neurons

The input capacitance of 30 BLA neurons was determined from the current response to a 10 mV hyperpolarizing voltage step from a holding potential of −60 mV. The mean membrane time constant value, τ_m, was 6.8 ± 0.5 ms and the input conductance, G_m, was 11.6 ± 1.0 nS, resulting in a mean calculated input capacitance, $C_m = G_m\tau_m$, of 69.7 ± 4.7 pF. The distribution of input capacitance values was unimodal, as shown in Fig. 2(c).

AMPA receptor-mediated evoked synaptic currents

EC stimulation in the presence of AP5, LY 293558, bicuculline and SCH 50911 at a holding potential of −70 mV elicited inward currents in BLA neurons. Responses to 25 successive stimuli applied at 10 s intervals were analyzed in five cells. The mean peak amplitude was 1674 ± 650 pA (range: 824–3972 pA), the half-width was 11.2 ± 2.0 ms, the 10–90% rise time was 3.5 ± 1.1 ms and the 90–10% decay time was 24.5 ± 4.5 ms. In these five cells, the mean latency to the peak response was 8.6 ± 1.8 ms (range: 5.5–14.8) and the peaks were well aligned with mean jitter of 429 ± 163 μs. The short latency and minimal jitter suggests that the responses are monosynaptic.

Switching the holding potential to more positive levels resulted in a decrease in the inward synaptic response and transition to net outward current at potentials positive to reversal potential values in the range of −35 to +15 mV (mean, −11.7 ± 4.0 mV). Current–voltage plots were generated by measuring the peak amplitude of the evoked synaptic response at different holding potentials. The RI was calculated by dividing the peak conductance at +40 mV by the peak conductance at −60 mV, as described by Ozawa *et al.* (1991). Figure 7 illustrates synaptic currents for typical inwardly and linearly rectifying neurons, along with current–voltage relationships of normalized peak current values for groups of both types of neurons. The distribution of RI values is shown in

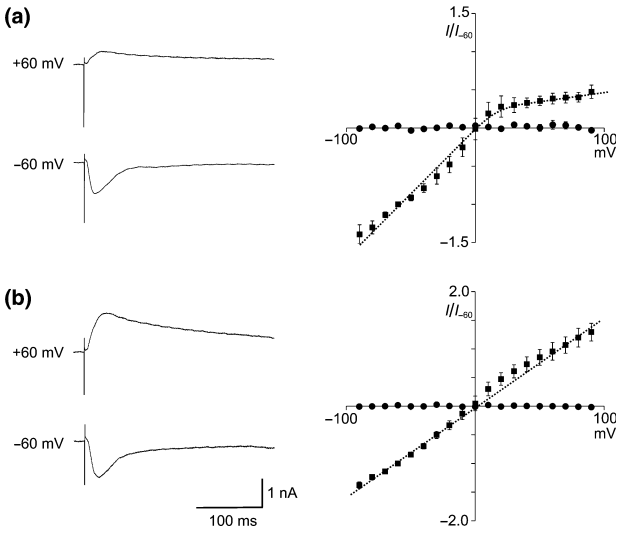

Fig. 7 AMPA receptor-mediated synaptic responses in BLA principal neurons exhibit both inwardly rectifying and linear current–voltage relationships. (a) Traces to left are typical synaptic responses evoked by EC stimulation in an inwardly rectifying neuron at holding potentials of −60 to +60 mV. The graph to the right plots the normalized mean ± SEM peak current amplitudes at holding potentials of −90 to +90 mV (10 mV increments) in inwardly rectifying neurons (rectification index <1) before (■, 10 neurons) and after (● three neurons) exposure to 50 μM GYKI 52466. For each cell, the peak current at each potential was normalized to the peak control current value at −60 mV. The fit to the data values was made by eye. (b) Similar to (a), except that linearly rectifying neurons were selected (five neurons before and one neuron after GYKI 52466).

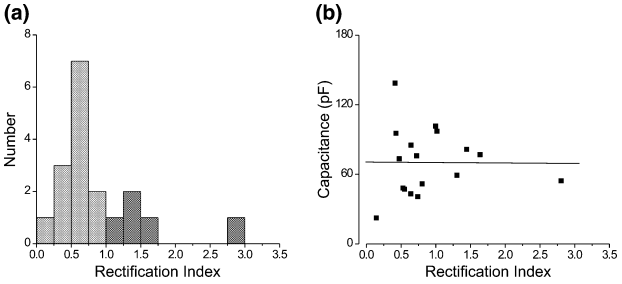

Fig. 8 (a) Distribution of rectification index values for 17 neurons. Lighter bars indicate inwardly rectifying neurons; darker bars are linear or outwardly rectifying neurons. (b) Scatter plot of rectification index against input capacitance for the same cells. The best fit straight line is shown. The slope is nearly 0 (−0.4 ± 11.8, $r = -0.01$), indicating no correlation between rectification index and capacitance.

Fig. 8(a) (range, 0.14–2.80; mean, 0.89 ± 0.15; $n = 17$). A total of 72% of cells had RI values <1, indicating inward rectification. Nearly all of these cells had RI values in the intermediate range (0.25–1.0); only one cell had a RI <0.25. As illustrated in Fig. 8(b), there was no correlation between cell input capacitance and the RI, indicating that neurons with small membrane surface areas do not preferentially exhibit inwardly rectifying AMPA receptor-mediated synaptic responses.

The polyamine-containing wasp toxin analog, philanthotoxin-343, has been shown to selectively inhibit inwardly rectifying AMPA receptor currents (Armstrong and MacVicar 2001). Accordingly, synaptic responses in three BLA principal neurons with rectification indexes in the intermediate range were inhibited after perfusion of the slice with 10 μM philanthotoxin-343.

Discussion

AMPA receptor responses in principal projection neurons in many forebrain regions, such as the hippocampus, neocortex and lateral amygdala, are linearly or outwardly rectifying and have low calcium permeability (Keller *et al*. 1991; Jonas and Sakmann 1992; Mahanty and Sah 1999; Weisskopf and LeDoux 1999). Functional studies of recombinant AMPA receptors expressed in heterologous cells indicate that the AMPA receptors generating these responses contain at least one edited GluR2 subunit (Verdoorn *et al*. 1991). In contrast, interneurons often exhibit inwardly-rectifying and calcium-permeable AMPA receptor responses; the predominant form of AMPA receptor in these cells is one that lacks an edited GluR2 subunit (Gilbertson *et al*. 1991; McBain and Dingledine 1993; Bochet *et al*. 1994; Jonas *et al*. 1994; Geiger *et al*. 1995, 1997; Jonas and Burnashev 1995; Isa *et al*. 1996; Tsuzuki *et al*. 2001; Sah and Lopez De Armentia 2003). Previous immunohistochemical studies have demonstrated that BLA neurons express various AMPA receptor subunits and, in particular, are stained with an antiserum that recognizes GluR2 and GluR3 (Farb *et al*. 1995; McDonald 1994; He *et al*. 1999).

In the present study, we found that most synapses in the BLA, in contrast to synapses onto hippocampal pyramidal neurons, did not exhibit GluR2 immunoreactivity. This is despite the fact that most BLA neurons express GluR2 immunoreactivity in their cell bodies and proximal dendrites. The antiserum we used was generated against a unique sequence in the carboxy terminus of rat GluR2 and has been demonstrated to bind specifically to GluR2 by western blot. The carboxy terminus of GluR2 is homologous to GluR3 but to no other known rat protein. Moreover, by western blot, the antiserum has been shown to cross-react weakly with GluR3. Therefore, we cannot exclude the possibility that some of the cell body/proximal dendritic labeling was to GluR3, although it seems unlikely that this represents a major fraction of the immunoreactivity. In fact, both GluR2 and GluR3 mRNA can be detected by *in situ* hybridization histochemistry in amygdala (Sato *et al*. 1993; Gold *et al*. 1997; Friedman *et al*. 2000). The high level of expression of GluR2 immunoreactivity at CA1 synapses is compatible with the observation of Wenthold *et al*. (1996) that AMPA receptors immunoprecipitated from the CA1 region of rat hippocampus (primarily

pyramidal neurons) nearly always contain GluR2, either with GluR1 or GluR3.

At synapses either in the hippocampus or amygdala, GluR2 immunoreactivity was exclusively localized to postsynaptic elements. Labeled synapses invariably had pronounced postsynaptic densities and were apposed to presynaptic terminals filled with round vesicles; such asymmetric (type 1) synapses are often glutamatergic. Postsynaptic densities were especially heavily labeled and, in spines and dendritic shafts exhibiting labeled synapses, reaction product often filled the entire membrane-delimited postsynaptic structure. Since immunoperoxidase is a diffusible marker, it is not possible to infer the precise localization of GluR2 within the postsynaptic structures or to conclude that GluR2 subunit protein is associated with synaptic elements (Baude *et al*. 1995). However, the results do demonstrate that GluR2 immunoreactivity in BLA is uniquely postsynaptic, a conclusion in line with that of Petralia *et al*. (1997) from immunoelectron microscopic studies of hippocampus, neocortex, cerebellum and spinal cord dorsal horn in which GluR2 antibody labeling was only on postsynaptic structures. These authors used the pre-embedding immunoperoxidase method, as in the present study, and also post-embedding immunogold, which provides more precise receptor localization. The immunogold and immunoperoxidase results were entirely consistent in demonstrating that GluR2 is largely or exclusively postsynaptic. Therefore, it seems unlikely that the immunoperoxidase technique as used in the present study would lead to erroneous conclusions regarding presynaptic versus postsynaptic localization. Our observation that GluR2 is exclusively present postsynaptically in BLA also confirms the prior immunoelectron microscopic study of Farb *et al*. (1995), using an antiserum that does not distinguish between GluR2 and GluR3, in which only one of 929 labeled synapses in the basal amygdala (a region largely coinciding with the BLA as we define it; see Gryder and Rogawski 2003) was over an axon terminal. These workers found that the antiserum stained both dendritic spines and dendritic shafts, but they did not specifically examine the frequency at which morphological synapses are labeled. He *et al*. (1999) detected a similar pattern of staining with a GluR2-selective monoclonal antibody.

The synapses we observed in the BLA were predominantly (86%) onto spines, which studies using Golgi staining (McDonald 1982) and intracellular labeling (Washburn and Moises 1992) have found are mainly present on principal neurons (spiny pyramidal class I cells) and not on interneurons (spine-sparse non-pyramidal class II cells). Golgi and retrograde labeling studies have demonstrated that interneurons represent only a small fraction (15%) of neurons within the BLA (McDonald 1992b). Moreover, interneurons are not evenly distributed within the nucleus but are clustered at the BLA border, near the boundary between the dorsolateral and ventromedial subdivisions of lateral amygdala and in the dorsal portion of posterior BLA (Millhouse and DeOlmos 1983; McDonald 1984). We collected our specimens for electron microscopy from the center of the nucleus to avoid these border zones containing interneuron clusters. These various considerations suggest that the majority of the synapses we observed in electron micrographs from the BLA were onto principal neurons, even though both principal neurons and interneurons in the BLA receive excitatory inputs.

Our conclusion from immunocytochemistry that BLA principal neuron synapses are GluR2 poor was supported by the results from electrophysiological recording in slices from juvenile rats. Our whole-cell voltage clamp recordings were carried out from large, visually identified neurons in the center of the region, presumed to correspond to the BLA, and were likely to be principal neurons. Some of these cells were identified as principal neurons by biocytin staining (not shown). In addition, they had high input capacitances, indicating large membrane surface areas, and the distribution of input capacitances was unimodal, suggesting that the recordings were from a single population of cells. Many neurons had RI values that were <1, indicating inward rectification. Ozawa *et al*. (1991) separated neurons into three classes based upon their RI values: 'type I' which have RI >1, 'type II' which have RI <0.25 and, 'intermediate', which have RI in the range 0.25–1. Rectification in the intermediate range is believed to reflect the co-existence of calcium-permeant and calcium-impermeant AMPA receptors (Iino *et al*. 1994). By these criteria, most (72%) of the neurons we recorded were intermediate (13 neurons) or type I (one neuron). While not all AMPA receptors in these neurons are likely to be calcium-permeable, a fraction certainly is. In fact, it has previously been demonstrated that calcium-permeant and calcium-impermeant AMPA receptors can co-exist in some cell types, including medial septal principal neurons (Armstrong and MacVicar 2001), superior colliculus neurons (Endo and Isa 2001), retinal ganglion cells (Zhang *et al*. 1995), avian cochlear nucleus neurons (Ravindranathan *et al*. 2000; Gardner *et al*. 2001), cerebellar stellate cells (Liu and Cull-Candy 2000), spinal motoneurons (Greig *et al*. 2000) and spinal dorsal horn neurons including projection neurons (Engelman *et al*. 1999). There is also evidence for such receptor heterogeneity in some hippocampal interneurons (He *et al*. 1998) and, through the use of polyamine toxins that selectively block GluR2-lacking AMPA receptors, it has been possible to demonstrate that synaptic responses in hippocampal interneurons are mediated by GluR2-lacking and GluR2-containing AMPA receptors that co-exist in the same cell (Washburn *et al*. 1997; Tóth and McBain 1998).

It has also been hypothesized that AMPA receptor subunits may assemble freely so as to produce cells with a uniform 'mosaic' of calcium-permeable and calcium-impermeable AMPA receptors, and that the extent to which AMPA

receptors are of the calcium-permeable type is inversely related to the quantity of GluR2 mRNA expressed by the cell (Burnashev *et al*. 1992; Geiger *et al*. 1995; Dingledine *et al*. 1999). Moreover, Washburn *et al*. (1997) have provided evidence that there could be a variable number of GluR2 subunits in AMPA receptors, and that while calcium permeability may be maximally reduced with the presence of a single GluR2 subunit in the heteromeric complex, larger numbers of GluR2 subunits per channel can produce additional alterations in channel function. Our results lead to a modification of these ideas somewhat, at least as they relate to the BLA. As noted above, immunohistochemical studies at the light level demonstrate that BLA neurons do express considerable GluR2 as is the case, for example, for spinal motoneurons which are believed to have a mixed population of AMPA receptors (Greig *et al*. 2000). However, since only a small proportion of synapses show GluR2 immunoreactivity, it appears that GluR2 containing AMPA receptors are not uniformly distributed to synaptic sites but rather, that GluR2 may be targeted selectively within the dendritic compartment. In fact, there is evidence that differential dendritic targeting of AMPA receptor subunits occurs in other cell types (Rubio and Wenthold 1997; Petralia *et al*. 1999, 2000). In addition, Liu and Cull-Candy (2000) have reported that somatic AMPA receptors in cerebellar stellate cells display properties characteristic of GluR2-containing assemblies, whereas synaptic AMPA receptors in these neurons appear to largely lack GluR2. In the case of BLA principal neurons, GluR2 protein is either restricted from translocating to many dendritic synapses or its turnover is enhanced at these sites. Indeed, evidence has recently been provided that GluR2 can be locally translated within dendrites from GluR2 mRNA (Kacharmina *et al*. 2000) to form functional receptors (Ju *et al*. 2004), raising the possibility that the GluR2 content of synaptic AMPA receptors can be regulated locally. Whether this or other mechanisms apply, it does appear that the GluR2 subunit content at synapses is highly plastic and can vary even in response to short-term changes in synaptic activity (Liu and Cull-Candy 2000, 2002). Therefore, the picture we have obtained of low GluR2 expression at BLA synapses could vary under different physiological circumstances.

It is interesting to note that there was no correlation between RI and cell input capacitance. Although morphologically heterogenous, presumed interneurons in the BLA (non-pyramidal stellate and fusiform cells) are smaller than principal neurons (McDonald 1982; Millhouse and DeOlmos 1983). Had we inadvertently recorded from some interneurons, these smaller (low capacitance) neurons should have had lower RI values. There was no indication that this was the case. The high abundance of intermediate-type neurons in the BLA is in contrast to the situation in hippocampus where the bulk of hippocampal pyramidal neurons had RI values in the type I range (86% for CA1 neurons, 61% for CA3 neurons, 76% for dentate gyrus; Isa *et al*. 1996) and, in these regions, the neurons in the intermediate range had RI values relatively close to 1.0. The fact that AMPA receptor currents in hippocampal pyramidal neurons generally exhibit little inward rectification is compatible with our observation and that of Petralia *et al*. (1997) that GluR2 is expressed at the majority of immunolabeled synapses in the CA1 and CA3 regions.

What are the functional consequences of the existence of a substantial fraction of GluR2-lacking, presumably calcium-permeable AMPA receptors in BLA principal neurons? It has been proposed that calcium-permeable AMPA receptors can participate in forms of synaptic plasticity when the receptors are tetanically activated (Gu *et al*. 1996; Mahanty and Sah 1998). The BLA exhibits various non-conventional forms of activity-dependent synaptic plasticity (Li *et al*. 1998; Li *et al.* 2001). The extent to which calcium-permeable AMPA receptors participate in these forms of synaptic plasticity require further exploration, although Mahanty and Sah (1998) have already reported that calcium-permeable AMPA receptors may mediate a non-NMDA receptor-dependent form of synaptic facilitation in BLA interneurons. In addition, the amygdala is highly susceptible to electrical stimulation-induced epileptogenesis; whether such 'kindling' is to some extent mediated by calcium-permeable AMPA receptors remains to be determined. Interestingly, however, Prince *et al*. (1995, 2002) have reported that the development of amygdaloid kindling is associated with a transient reduction of GluR2 protein expression specifically in the piriform cortex/amygdaloid region. Thus, the induction of the kindling process may be associated with an enhancement of plasticity mechanisms dependent upon calcium-permeable AMPA receptors. Finally, calcium-permeable AMPA receptors could contribute to the high vulnerability of amygdala neurons to seizure-induced damage (Pitkänen *et al*. 1998) in the same way that such receptors enhance the vulnerability of spinal motoneurons (Van Damme *et al*. 2002; Kawahara *et al*. 2003). These mechanisms may be enhanced in a variety of circumstances, including status epileptics and brain ischemia, by further reductions in GluR2 (Gorter *et al*. 1997; Pellegrini-Giampietro *et al*. 1997; Tanaka *et al*. 2000; Sommer *et al*. 2001).

Acknowledgements

We are grateful to Susan J.-H. Tao Cheng, Ph.D. for assistance with the electron microscopy. This work utilized the resources of the NINDS Electron Microscopy Facility.

References

Armstrong J. N. and MacVicar B. A. (2001) Theta-frequency facilitation of AMPA receptor-mediated synaptic currents in the principal cells of the medial septum. *J. Neurophysiol.* **85**, 1709–1718.

Baude A., Nusser Z., Molnar E., McIlhinney R. A. and Somogyi P. (1995) High-resolution immunogold localization of AMPA type glutamate receptor subunits at synaptic and non-synaptic sites in rat hippocampus. *Neuroscience* **69**, 1031–1055.

Bochet P., Audinat E., Lambolez B., Crépel F., Rossier J., Iino M., Tsuzuki K. and Ozawa S. (1994) Subunit composition at the single-cell level explains functional properties of a glutamate-gated channel. *Neuron* **12**, 383–388.

Burnashev N., Monyer H., Seeberg P. H. and Sakmann B. (1992) Divalent ion permeability of AMPA receptor channels is dominated by the edited form of a single subunit. *Neuron* **8**, 189–198.

Dingledine R., Borges K., Bowie D. and Traynelis S. F. (1999) The glutamate receptor ion channels. *Pharmacol. Rev.* **51**, 7–61.

Donevan S. D. and Rogawski M. A. (1995) Intracellular polyamines mediate inward rectification of Ca^{2+}-permeable α-amino-3-hydroxy-5-methyl-4-isoxazolepropionic acid receptors. *Proc. Natl Acad. Sci. USA* **92**, 9298–9302.

Endo T. and Isa T. (2001) Functionally different AMPA-type glutamate receptors in morphologically identified neurons in rat superficial superior colliculus. *Neuroscience* **108**, 129–141.

Engelman H. S., Allen T. B. and MacDermott A. B. (1999) The distribution of neurons expressing calcium-permeable AMPA receptors in the superficial laminae of the spinal cord dorsal horn. *J. Neurosci.* **19**, 2081–2089.

Farb C. R., Aoki C. and Ledoux J. E. (1995) Differential localization of NMDA and AMPA receptor subunits in the lateral and basal nuclei of the amygdala: a light and electron microscopic study. *J. Comp. Neurol.* **362**, 86–108.

Friedman L. K., Belayev L., Alfonso O. F. and Ginsberg M. D. (2000) Distribution of glutamate and preproenkephalin messenger RNAs following transient focal cerebral ischemia. *Neuroscience* **95**, 841–857.

Gardner S. M., Trussell L. O. and Oertel D. (2001) Correlation of AMPA receptor subunit composition with synaptic input in the mammalian cochlear nuclei. *J. Neurosci.* **21**, 7428–7437.

Gean P. W. and Chang F. C. (1992) Pharmacological characterization of excitatory synaptic potentials in rat basolateral amygdaloid neurons. *Synapse* **11**, 1–9.

Geiger J. R., Melcher T., Koh D. S., Sakmann B., Seeburg P. H., Jonas P. and Monyer H. (1995) Relative abundance of subunit mRNAs determines gating and Ca^{2+} permeability of AMPA receptors in principal neurons and interneurons in rat CNS. *Neuron* **15**, 193–204.

Geiger J. R., Lubke J., Roth A., Frotscher M. and Jonas P. (1997) Submillisecond AMPA receptor-mediated signaling at a principal neuron-interneuron synapse. *Neuron* **18**, 1009–1023.

Gilbertson T. A., Scobey R. and Wilson M. (1991) Permeation of calcium ions through non-NMDA glutamate channels in retinal bipolar cells. *Science* **251**, 1613–1615.

Gold S. J., Ambros-Ingerson J., Horowitz J. R., Lynch G. and Gall C. M. (1997) Stoichiometries of AMPA receptor subunit mRNAs in rat brain fall into discrete categories. *J. Comp. Neurol.* **385**, 491–502.

Gorter J. A., Petrozzino J. J., Aronica E. M., Rosenbaum D. M., Opitz T., Bennett M. V. L., Connor J. A. and Zukin R. S. (1997) Global ischemia induces downregulation of GluR2 mRNA and increases AMPA receptor-mediated Ca^{2+} influx in hippocampal CA1 neurons of gerbil. *J. Neurosci.* **17**, 6179–6188.

Greig A., Donevan S. D., Mujtaba T. J., Parks T. N. and Rao M. S. (2000) Characterization of the AMPA-activated receptors present on motoneurons. *J. Neurochem.* **74**, 179–191.

Gryder D. and Rogawski M. A. (2003) Selective antagonism of GluR5 kainate receptor-mediated synaptic currents by topiramate in rat basolateral amygdala neurons. *J. Neurosci.* **23**, 7069–7074.

Gu J. G., Albuquerque C., Lee C. J. and MacDermott A. B. (1996) Synaptic strengthening through activation of Ca^{2+}-permeable AMPA receptors. *Nature* **381**, 793–796.

Hall R. A., Hansen A., Andersen P. H. and Soderling T. R. (1997) Surface expression of the AMPA receptor subunits GluR1, GluR2, and GluR4 in stably transfected baby hamster kidney cells. *J. Neurochem.* **68**, 625–630.

He Y., Janssen W. G., Vissavajjhala P. and Morrison J. H. (1998) Synaptic distribution of GluR2 in hippocampal GABAergic interneurons and pyramidal cells: a double-label immunogold analysis. *Exp. Neurol.* **150**, 1–13.

He Y., Janssen W. G. and Morrison J. H. (1999) Differential synaptic distribution of the AMPA-GluR2 subunit on GABAergic and non-GABAergic neurons in the basolateral amygdala. *Brain Res.* **827**, 51–62.

Iino M., Mochizuki S. and Ozawa S. (1994) Relationship between calcium permeability and rectification properties of AMPA receptors in cultured rat hippocampal neurons. *Neurosci. Lett.* **173**, 14–16.

Isa T., Itazawa S., Iino M., Tsuzuki K. and Ozawa S. (1996) Distribution of neurones expressing inwardly rectifying and Ca^{2+}-permeable AMPA receptors in rat hippocampal slices. *J. Physiol.* **491**,3, 719–733.

Janssens N. and Lesage A. S. J. (2001) Glutamate receptor subunit expression in primary neuronal and secondary glial cultures. *J. Neurochem.* **7**, 1457–1474.

Jonas P. and Sakmann B. (1992) Glutamate receptor channels in isolated patches from CA1 and CA3 pyramidal cells of rat hippocampal slices. *J. Physiol.* **455**, 143–171.

Jonas P. and Burnashev N. (1995) Molecular mechanisms controlling calcium entry through AMPA-type glutamate receptor channels. *Neuron* **15**, 987–990.

Jonas P., Racca C., Sakmann B., Seeburg P. H. and Monyer H. (1994) Differences in Ca^{2+} permeability of AMPA-type glutamate receptor channels in neocortical neurons caused by differential GluR-B subunit expression. *Neuron* **12**, 1281–1289.

Ju W., Morishita W., Tsui J., Gaietta G., Deerinck T. J., Adams S. R., Garner C. C., Tsien R. Y., Ellisman M. H. and Malenka R. C. (2004) Activity-dependent regulation of dendritic synthesis and trafficking of AMPA receptors. *Nat. Neurosci.* **7**, 244–253.

Kacharmina J. E., Job C., Crino P. and Eberwine J. (2000) Stimulation of glutamate receptor protein synthesis and membrane insertion within isolated neuronal dendrites. *Proc. Natl Acad. Sci. USA* **97**, 11 545–11 550.

Kamboj S. K., Swanson G. T. and Cull-Candy S. G. (1995) Intracellular spermine confers rectification on rat calcium-permeable AMPA and kainate receptors. *J. Physiol.* **486**, 297–303.

Kawahara Y., Kwak S., Sun H., Ito K., Hashida H., Aizawa H., Jeong S. Y. and Kanazawa I. (2003) Human spinal motoneurons express low relative abundance of GluR2 mRNA: an implication for excitotoxicity in ALS. *J. Neurochem.* **85**, 680–689.

Keller B. U., Konnerth A. and Yaari Y. (1991) Patch clamp analysis of excitatory synaptic currents in granule cells of rat hippocampus. *J. Physiol.* **435**, 275–293.

Li H. and Rogawski M. A. (1998) GluR5 kainate receptor mediated synaptic transmission in rat basolateral amygdala *in vitro*. *Neuropharmacology* **37**, 1279–1286.

Li H., Weiss S. R., Chuang D. M., Post R. M. and Rogawski M. A. (1998) Bidirectional synaptic plasticity in the rat basolateral amygdala: characterization of an activity-dependent switch sensitive to the presynaptic metabotropic glutamate receptor antagonist 2S-α-ethylglutamic acid. *J. Neurosci.* **18**, 1662–1670.

Li H., Chen A., Xing G., Wei M. and Rogawski M. A. (2001) Kainate receptor-mediated heterosynaptic facilitation in the amygdala. *Nat. Neurosci.* **4**, 612–620.

Liu S. Q. J. and Cull-Candy S. G. (2000) Synaptic activity at calcium-permeable AMPA receptors induces a switch in receptor subtype. *Nature* **405**, 454–458.

Liu S. J. and Cull-Candy S. G. (2002) Activity-dependent change in AMPA receptor properties in cerebellar stellate cells. *J. Neurosci.* **22**, 3881–9388.

Mahanty N. K. and Sah P. (1998) Calcium-permeable AMPA receptors mediate long-term potentiation in interneurons in the amygdala. *Nature* **394**, 683–687.

Mahanty N. K. and Sah P. (1999) Excitatory synaptic inputs to pyramidal neurons of the lateral amygdala. *Eur. J. Neurosci.* **11**, 1217–1222.

McBain C. J. and Dingledine R. (1993) Heterogeneity of synaptic glutamate receptors on CA3 stratum-radiatum interneurones of rat hippocampus. *J. Physiol.* **462**, 373–392.

McDonald A. J. (1982) Neurons of the lateral and basolateral amygdaloid nuclei: a Golgi study in the rat. *J. Comp. Neurol.* **212**, 293–312.

McDonald A. J. (1984) Neuronal organization of the lateral and basolateral amygdaloid nuclei in the rat. *J. Comp. Neurol.* **222**, 589–606.

McDonald A. J. (1992a) Cell types and intrinsic connections of the amygdala, in *The Amygdala* (Aggleton J. P., ed.), pp. 67–96. Wiley-Liss, New York.

McDonald A. J. (1992b) Projection neurons of the basolateral amygdala: a correlative Golgi and retrograde tract tracing study. *Brain Res. Bull.* **28**, 179–185.

McDonald A. J. (1994) Neuronal localization of glutamate receptor subunits in the basolateral amygdala. *Neuroreport* **6**, 13–16.

McDonald A. J. (1996) Localization of AMPA glutamate receptor subunits in subpopulations of non-pyramidal neurons in the rat basolateral amygdala. *Neurosci. Lett.* **208**, 175–178.

Millhouse O. E. and DeOlmos J. (1983) Neuronal configurations in lateral and basolateral amygdala. *Neuroscience* **10**, 1269–1300.

Ozawa S., Iino M. and Tsuzuki K. (1991) Two types of kainate response in cultured rat hippocampal neurons. *J. Neurophysiol.* **66**, 2–11.

Pellegrini-Giampietro D. E., Gorter J. A., Bennett M. V. L. and Zukin S. R. (1997) The GluR2 hypothesis: Ca^{2+}-permeable AMPA receptors in neurological disorders. *Trends Neurosci.* **20**, 464–470.

Petralia R. S., Wang Y.-X., Mayat E. and Wenthold R. J. (1997) Glutamate receptor subunit 2-selective antibody shows a differential distribution of calcium-impermeable AMPA receptors among populations of neurons. *J. Comp. Neurol.* **385**, 456–476.

Petralia R. S., Rubio M. E. and Wenthold R. J. (1999) Cellular and subcellular distribution of glutamate receptors, in *Handbook of Experimental Pharmacology: Ionotropic Glutamate Receptors in the CNS* (Jonas P. and Monyer H., eds), pp. 143–171. Springer-Verlag, New York.

Petralia R. S., Rubio M. E., Wang Y.-X. and Wenthold R. J. (2000) Regional and synaptic expression of ionotropic glutamate receptors, in *Handbook of Chemical Neuroanatomy: Glutamate* (Ottersen O. P. and Storm-Mathisen J., eds), pp. 145–182. Elsevier Science, New York.

Pitkänen A., Tuunanen J., Kälviäinen R., Partanen K. and Salmenperä T. (1998) Amygdala damage in experimental and human temporal lobe epilepsy. *Epilepsy Res.* **32**, 233–253.

Prince H. C., Tzingounis A. V., Levey A. I. and Conn P. J. (2002) Functional downregulation of GluR2 in piriform cortex of kindled animals. *Synapse* **38**, 489–498.

Prince H. K., Conn P. J., Blackstone C. D., Huganir R. L. and Levey A. I. (1995) Down-regulation of AMPA receptor subunit GluR2 in amygdaloid kindling. *J. Neurochem.* **64**, 462–465.

Rainnie D. G., Asprodini E. K. and Shinnick-Gallagher P. (1991) Excitatory transmission in the basolateral amygdala. *J. Neurophysiol.* **66**, 986–998.

Ravindranathan A., Donevan S. D., Sugden S. G., Greig A., Rao M. S. and Parks T. N. (2000) Contrasting molecular composition and channel properties of AMPA receptors on chick auditory and brainstem motor neurons. *J. Physiol.* **523**, 667–684.

Rubio M. E. and Wenthold R. J. (1997) Glutamate receptors are selectively targeted to postsynaptic sites in neurons. *Neuron* **18**, 939–950.

Sah P. and Lopez De Armentia M. (2003) Excitatory synaptic transmission in the lateral and central amygdala. *Ann. N.Y. Acad. Sci.* **985**, 67–77.

Sato K., Kiyama H. and Tohyama M. (1993) The differential expression patterns of messenger RNAs encoding non-*N*-methyl-D-aspartate glutamate receptor subunits (GluR1–4) in the rat brain. *Neuroscience* **52**, 515–539.

Sommer C., Roth S. U. and Kiessling M. (2001) Kainate-induced epilepsy alters protein expression of AMPA receptor subunits GluR1, GluR2 and AMPA receptor binding protein in the rat hippocampus. *Acta Neuropathol.* **101**, 460–468.

Swanson L. W. and Petrovich G. D. (1998) What is the amygdala? *Trends Neurosci.* **21**, 323–331.

Tanaka H., Grooms S. Y., Bennett M. V. and Zukin R. S. (2000) The AMPAR subunit GluR2: still front and center-stage. *Brain Res.* **886**, 190–207.

Tóth K. and McBain C. J. (1998) Afferent-specific innervation of two distinct AMPA receptor subtypes on single hippocampal interneurons. *Nat. Neurosci.* **1**, 572–578.

Tsuzuki K., Lambolez B., Rossier J. and Ozawa S. (2001) Absolute quantification of AMPA receptor subunit mRNAs in single hippocampal neurons. *J. Neurochem.* **77**, 1650–1659.

Van Damme P., Van Den Bosch L., Van Houtte E., Callewaert G. and Robberecht W. (2002) GluR2-dependent properties of AMPA receptors determine the selective vulnerability of motor neurons to excitotoxicity. *J. Neurophysiol.* **88**, 1279–1287.

Verdoorn T. A., Burnashev N., Monyer H., Seeburg P. H. and Sakmann B. (1991) Structural determinants of ion flow through recombinant glutamate receptor channels. *Science* **252**, 1715–1718.

Vissavajjhala P., Janssen W. G., Hu Y., Gazzaley A. H., Moran T., Hof P. R. and Morrison J. H. (1996) Synaptic distribution of the AMPA-GluR2 subunit and its colocalization with calcium-binding proteins in rat cerebral cortex: an immunohistochemical study using a GluR2-specific monoclonal antibody. *Exp. Neurol.* **142**, 296–312.

Washburn M. S. and Moises H. C. (1992) Electrophysiological and morphological properties of rat basolateral amygdaloid neurons *in vitro*. *J. Neurosci.* **12**, 4066–4079.

Washburn M. S., Numberger M., Zhang S. and Dingledine R. (1997) Differential dependence on GluR2 expression of three characteristic features of AMPA receptors. *J. Neurosci.* **17**, 9393–9406.

Weisskopf M. G. and LeDoux J. E. (1999) Distinct populations of NMDA receptors at subcortical and cortical inputs to principal cells of the lateral amygdala. *J. Neurophysiol.* **81**, 930–934.

Wenthold R. J., Petralia R. S., Blahos J. I. I. and Niedzielski A. S. (1996) Evidence for multiple AMPA receptor complexes in hippocampal CA1/CA2 neurons. *J. Neurosci.* **16**, 1982–1989.

Yoshioka A., Ikegaki N., Williams M. and Pleasure D. (1996) Expression of *N*-methyl-D-aspartate (NMDA) and non-NMDA glutamate receptor genes in neuroblastoma, medulloblastoma, and other cells lines. *J. Neurosci. Res.* **46**, 164–178.

Zhang D., Sucher N. J. and Lipton S. A. (1995) Co-expression of AMPA/kainate receptor-operated channels with high and low Ca^{2+} permeability in single rat retinal ganglion cells. *Neuroscience* **67**, 177–188.